

# Design of a heterotetrameric coiled coil

Benjamin C. Root, Laurel D. Pellegrino, Emily D. Crawford,  
Bashkim Kokona, and Robert Fairman\*

Department of Biology, Haverford College, Haverford, Pennsylvania 19041

Received 23 June 2008; Revised 25 October 2008; Accepted 3 November 2008

DOI: 10.1002/pro.30

Published online 2 December 2008 proteinscience.org

**Abstract:** We have successfully designed a simple peptide sequence that forms highly stable coiled-coil heterotetramers. Our model system is based on the GCN4-pLI parallel coiled-coil tetramer, first described by Kim and coworkers (Harbury *et al.*, *Science* 1993;262:1401–1407). We introduced glutamates at all of the *e* and *c* heptad positions of one sequence (ecE) and lysines at the same positions in a second sequence (ecK). Based on a modeling study, these sidechains are close enough in space to form structure-stabilizing salt bridges. We show that ecE and ecK are highly unstable by themselves but form very stable parallel helical tetramers when mixed, as judged by circular dichroism, analytical ultracentrifugation, and disulfide crosslinking studies. The origin of the difference in stabilities between the homomeric structures and the heteromeric structures comes from a combination of the relief of electrostatic repulsions with concomitant formation of electrostatic attractive interactions based on pH and NaCl screening experiments. We quantify the stability of the heterotetrameric coiled coil from a thermodynamic analysis and compare the finding to other similar coiled-coil systems.

**Keywords:** coiled coil; heterotetramer; protein design; electrostatic interactions; analytical ultracentrifugation; circular dichroism

## Introduction

Coiled coils have provided a simple model system for protein engineering studies and the development of biotechnology reagents and novel biomaterials. These motifs are characterized by two or more helices supercoiled about one another resulting in a slight underwinding of each individual helix such that there are 3.5 residues per turn of helix. Thus, seven residue positions define two turns of a helix and the positions are labeled by convention with the letters, *a–g*. Two positions, *a* and *d*, are typically hydrophobic as they are usually fully desolvated as the helices come together. Stability and specificity is also influenced by

residues at the other five positions, but do not play nearly as important a role as the *a* and *d* positions in folding. Nevertheless, many protein design efforts have taken advantage of these other positions, particularly the partially desolvated *e* and *g* positions, to define specificity of oligomerization and helix pairing.

We have been interested in designing heterospecificity into tetrameric coiled coils for their potential in biomaterials research.<sup>1</sup> Electrostatic interactions are well documented in the literature for introducing heterospecificity into coiled-coil pairing interactions and have been reviewed recently.<sup>2,3</sup> Although many examples exist in using salt bridges to engineer specificity into dimeric coiled coils, there are only a few examples of similar approaches for tetrameric coiled coils. Earlier work in our laboratory showed that glutamates and lysines could be engineered into the well-solvated heptad positions, *b* and *c*, in peptides containing the lac repressor tetramerization domain to create salt-bridge induced heterotetramers.<sup>4</sup> We showed that this model system contained antiparallel helices. Heterospecificity has also been engineered into a parallel tetrameric coiled coil, called Acid-pLL/Base-pLL, using

---

*Abbreviations:* ANS, 1-anilinonaphthalene-8-sulfonate; CD, circular dichroism spectropolarimetry; RP-HPLC, reversed phase-high performance liquid chromatography; SE, sedimentation equilibrium; SV, sedimentation velocity; TFA, trifluoroacetic acid.

Grant sponsor: NSF; Grant numbers: MCB-0211754, MCB-0516025.

\*Correspondence to: Robert Fairman, Robert Fairman, Department of Biology, Haverford College, 370 Lancaster Avenue, Haverford, PA 19041. E-mail: rfairman@haverford.edu

the well-known GCN4 coiled-coil system.<sup>5-7</sup> In this work, charged residues were introduced at *e* and *g* heptad positions of the GCN4 coiled-coil sequence, and these mutations, in conjunction with replacement of a buried asparagine residue with a leucine residue (at an *a* heptad position) revealed the formation of heterotetramers. This structure was highly stable yet lacked specificity of helix orientation. Other studies, in which charged residues are introduced at *e* and *g* positions of different coiled-coil model sequences, revealed a preference for dimerization,<sup>8,9</sup> leading to some question as to the generality of this approach to designing heterotetramers.

We wanted to engineer heterospecificity into a parallel coiled-coil model system already predetermined to form tetramers to avoid some of the specificity issues described earlier, and so we took an advantage of other design work from the Kim lab in which it was shown that leucines and isoleucines placed at the *a* and *d* positions, respectively, specified the formation of highly stable and highly specific tetramers.<sup>10</sup> This work and another work by Hill *et al.*<sup>11</sup> have shown that selective incorporation of hydrophobic residues other than leucine in the hydrophobic core of coiled-coil structures can avoid problems with ill-defined, or dynamic, helical orientations.<sup>12</sup> Other details of our design strategy are described later.

## Results and Discussion

We used the crystal structure of GCN4-pLI, a parallel tetrameric coiled coil,<sup>10</sup> to evaluate which pair of positions in the coiled-coil repeating unit would best foster charged interactions between glutamate and lysine residues. We first considered interactions between *b* and *c'* positions as modeling studies indicated the potential role of such interactions in coiled-coil structure,<sup>13</sup> and our previous work on the lac repressor antiparallel coiled coil showed that interhelical interactions can influence heterospecificity.<sup>4,14</sup> However, we ruled out using such pair-wise interactions between positions *b* and *c'* for our current design efforts since this earlier work revealed that, while stabilizing, such interactions were highly solvated, and thus easily screened with salts. Looking at these equivalent heptad positions in the GCN4-pLI crystal structure confirmed that these positions are indeed highly solvated. We also ruled out pair-wise interactions at *e* and *g'* positions because amino acids at these positions are significantly desolvated and could lead instead to significant destabilization of a designed heterotetramer. In fact, charged residues at these positions are often seen acting to stabilize dimeric coiled coils and can be introduced at these positions to disfavor higher order oligomeric states.<sup>8,9</sup> Thus, a compromise must be sought between these design issues. We considered instead pair-wise interactions between *b* and *g'* positions and *c* and *e'* positions. Charged residues are allowed at the partially

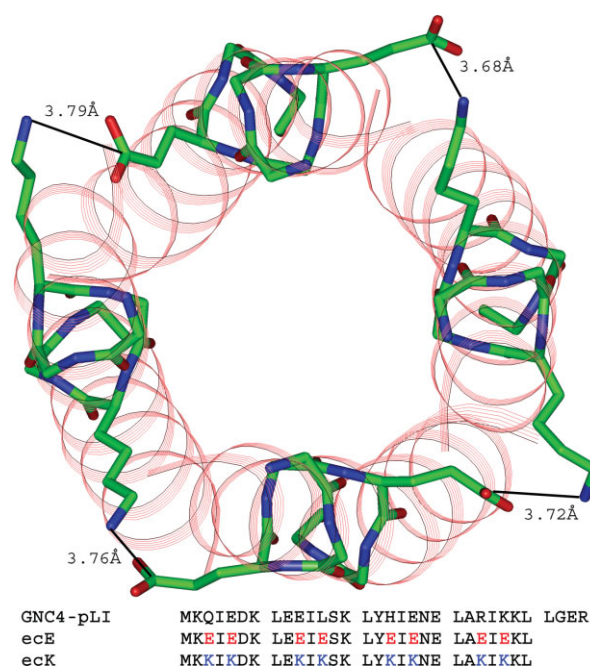


**Figure 1.** Backbone representation of the coiled coil highlighting single glu-lys salt-bridges between individual chains. The sidechains were energy minimized as described in the Materials and Methods and the distances between the carboxy and amino groups after energy minimization are highlighted. The peptide sequences are shown for the parent peptide GCN4-pLI, ecE, and ecK, with substitutions color-highlighted.

buried *e* and *g* positions as seen in GCN4-pLI; the degree to which these residues, even in the absence of sidechain interactions, affect protein stability has not been quantified. We used InsightII to introduce glutamic acid and lysine residues at either *b* and *g'* or *c* and *e'* sites (see Fig. 1 for *c, e'* site substitutions) in their preferred rotamer conformations. More specifically, glutamic acid residues were substituted into all *c* and *e* positions (or all *b* and *g* positions) of one helix and lysine residues were substituted into all *c* and *e* positions (or all *b* and *g* positions) of a neighboring helix in order to measure the distance between their functional groups. We then minimized the structure, as described in Materials and Methods, to make sure that there was no steric clashing. To facilitate analysis, we had to do multiple rounds of manual bond rotation and minimization to optimize the distances between these residues. We found that the carboxyl and amino functional groups of the glutamate and lysine residues, respectively, could be placed within 3.78 Å (for *c, e'* pairs) and 3.68 Å (for *b, g'* pairs) of one another (by measuring the distance between heavy atoms), or close to the optimal distance expected for salt bridge formation. We chose to utilize *e* and *c* sites, rather than *b* and *g* sites, in our peptides because there are five possible *c-e'* interactions and only four possible *b-g'* interactions in GCN4-pLI. Additionally, this design

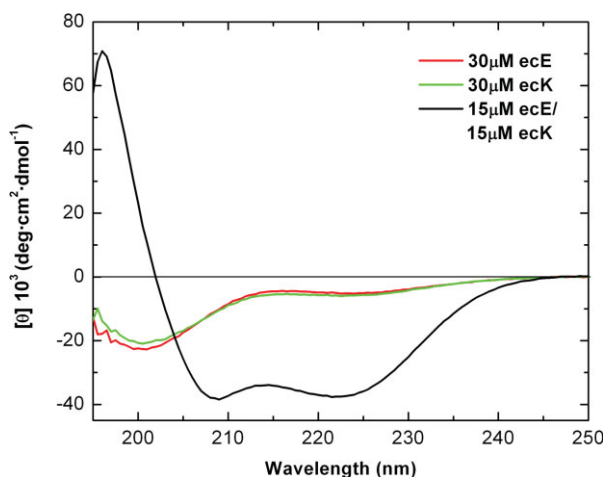


**Figure 2.** Circular dichroism spectra of ecE and ecK peptides were collected either individually (dashed and dashed/dotted lines) or as a 1:1 mixture (solid line). Samples were prepared in 10 mM phosphate, pH 7.5, and 150 mM NaCl at 25°C.

choice left a tyrosine residue in the peptide that facilitated determination of peptide concentrations in solution.<sup>15</sup> We synthesized and purified two peptides containing either glutamates (ecE) or lysines (ecK) at the *c* and *e* positions and their sequences are shown in Figure 1. The peptides were acetylated at the amino terminus and amidated at the carboxy terminus.

We hypothesized that the two peptides would remain unfolded when studied separately due to inter-helical electrostatic repulsions between like-charged residues at the *e* and *c'* sites, but when mixed would form a stable heterotetrameric coiled-coil structure. We used circular dichroism (CD) to test for helical content as a measure of coiled-coil formation. CD spectra were acquired for ecE, ecK, or an equimolar ecE/ecK mixture (all at 30 μM total peptide concentration) in 10 mM sodium phosphate pH 7.5 and 150 mM NaCl (see Fig. 2). The spectra of ecE and ecK showed that both peptides were largely unfolded when separate, with strong minima at 202 nm and very weak minima at 222 nm. The predicted helix content, as measured by the band intensity at 222 nm, using the method described by Baldwin's laboratory was 15%.<sup>16</sup> The equimolar ecE/ecK mixture, on the other hand, was judged to be fully helical, with the 202 nm minimum shifted to 208 nm and the minimum at 222 nm of approximately equal intensity to the 208 nm minimum. The helix content for this spectrum was calculated to be 99%.

To determine the size of the ecE and ecK peptides separately, or in a 1:1 mixture, we ran both sedimentation velocity (SV) and sedimentation equilibrium (SE) experiments. SV data, collected using 400 μM peptide, indicate that the ecE/ecK complex sediments as a single species with an  $s_{20,w}$  value of 1.4 S and a  $D_{20,w}$

value of  $1.18 \times 10^{-6} \text{ cm}^2 \text{ s}^{-1}$  [Fig. 3(A)]. When coupled, these values give a molecular mass of 12,650 Da, which is within 8.1% of the theoretical value of 13,778 Da (for comparison, ribonuclease, which has a  $D_{20,w}$  value of  $1.19 \times 10^{-6} \text{ cm}^2 \text{ s}^{-1}$ , has a molecular mass of 13,683 Da). The ecE and ecK peptides separately were too small to analyze accurately with SV, and so we turned to SE analysis to determine their oligomeric states. Data were collected at three rotor speeds using a peptide concentration of 30 μM in 10 mM sodium phosphate 7.3 and 150 mM NaCl, and the data were combined for global analysis to determine the apparent molecular masses. Single species analysis of the data show that ecE and ecK are predominantly monomeric (Table I). The ecK peptide shows a slightly elevated apparent molecular mass and model analysis suggests that this peptide weakly associates at this concentration. On the other hand, the ecE/ecK mixture gives an average molecular mass consistent with that of a heterotetramer [Table I and Fig. 3(B)]. Model analysis confirms this conclusion (Table II). The best fit single species model is that of a heterotetramer; however, there is a slight improvement in the fits using a monomer-tetramer model, in which the monomer is approximated as an average of the theoretical masses of the ecE or ecK peptides. It is unlikely though, based on stability studies (described later), that any monomer present is due to a monomer-tetramer equilibrium. Rather, evidence for small amounts of monomer most likely reflects a difference in the two peptide concentrations resulting in one peptide being in slight excess.

The lack of specificity in the related structure described by Lumb and Kim<sup>5</sup> led us to test if the our coiled-coil system might be dynamic, or have molten globule-like characteristics, and be ill-determined in the helix orientation. We tested for these characteristics first by looking for binding of the hydrophobic dye, 1-anilino-naphthalene-8-sulfonate (ANS), which has been shown to bind selectively to molten globule-like proteins.<sup>17</sup> We saw no ANS fluorescence in the presence of ecE/ecK at a peptide monomer concentration of 6 μM (see Fig. 4). This result was compared with binding of ANS to two proteins: lysozyme (a well-folded protein) and apomyoglobin (known to have molten globule characteristics). Binding of ANS to apomyoglobin results in a huge increase in fluorescence relative to the other proteins and reflects the dequenching of fluorescence that occurs when ANS is in a more hydrophobic environment (as mimicked by the fluorescence seen in ethanol, a more nonpolar solvent; Fig. 4). It is possible that ANS could bind weakly to the ecE/ecK heterotetramer, as shown by Lumb and Kim<sup>5</sup> for their designed heterotetramer, Acid-pLL/Base-pLL; however, peptide concentrations up to 150 μM resulted in no increase in fluorescence. This difference in ANS binding is likely explained by the differences in the core residues: Acid-pLL/Base-pLL

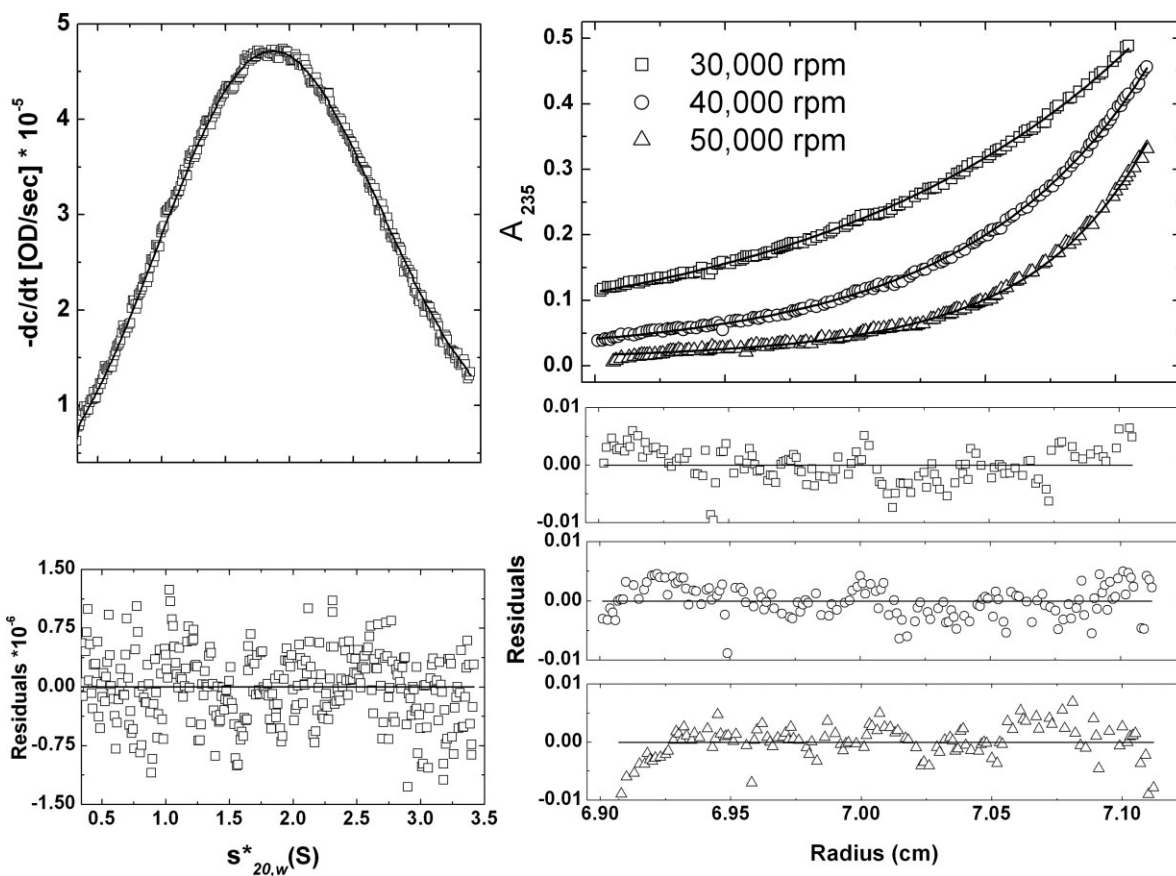


**Figure 3.** Determination of oligomeric state by analytical ultracentrifugation. **(A)** Sedimentation velocity experiments were prepared using 400  $\mu\text{M}$  peptide monomer concentration in 10 mM phosphate, pH 7.3, 150 mM NaCl at 25°C. The data are shown fit with a single species with an  $s_{20,w} = 1.400 \pm 0.001$  S and a  $D_{20,w} = 11.81 \pm 0.03 \times 10^{-7}$   $\text{cm}^2 \text{s}^{-1}$ . The residuals from fitting of the model to the data are shown below. **(B)** Sedimentation equilibrium experiments were run at 30,000, 40,000, and 50,000 rpm. The solution conditions are identical to the SV experiment described in A) except that the peptide concentration was 30  $\mu\text{M}$  (on a per monomer basis). The data at all three speeds are shown fit with a single species model in which the molecular mass was a fitting parameter. The residuals from fitting of the model to the data for each speed are shown below for 50,000 rpm (top), 40,000 rpm (middle), and 30,000 rpm (bottom).

contains leucines at both core, *a* and *d*, heptad positions, whereas our heterotetramer is based on GCN4-pLL, in which packing interactions in the core are thought to be more specific for an antiparallel heterotetramer.

We then tested for specificity of helix orientation. We adapted a protocol developed by the Kim laboratory to test for helix orientation in their Acid-pLL/

**Table I.** Sedimentation Equilibrium Analysis of *ecE* and *ecK* Peptides

Peptide (30 $\mu\text{M}$ )	Theoretical molecular mass (Da)	Experimental molecular mass <sup>a</sup> (Da)
<i>ecE</i>	3450.9	3470 $\pm$ 350
<i>ecK</i>	3443.4	6330 $\pm$ 580
<i>ecE/ecK</i>	13,789	12940 $\pm$ 580

<sup>a</sup> The experimental molecular masses are determined from global fits to the data collected at 30 000, 40 000, and 50 000 rpm at 25°C in 10 mM phosphate buffer and 150 mM NaCl at pH 7.3.

Base-pLL, using a disulfide crosslinking approach.<sup>5</sup> We synthesized two variants of our *ecK* peptide, one containing the sequence, WCGG, at the amino terminus (*ecK<sub>N</sub>*) and a second containing the sequence, GGC, at the carboxy terminus (*ecK<sub>C</sub>*). Depending on the

**Table II.** Model Analysis of Sedimentation Equilibrium Data for the *ecE/ecK* Complex

Model	SROV <sup>a</sup>
Single species	3.37
Monomer	25.8
Dimer	16.23
Trimer	7.35
Tetramer	3.9
Hexamer	3.90
1 $\rightarrow$ 2	17.31
1 $\rightarrow$ 3	9.23
1 $\rightarrow$ 4	2.91
1 $\rightarrow$ 5	3.25

<sup>a</sup> Square root of variance ( $\times 10^{-3}$ ) of the model calculated from global fitting to the data collected as described in Table I.

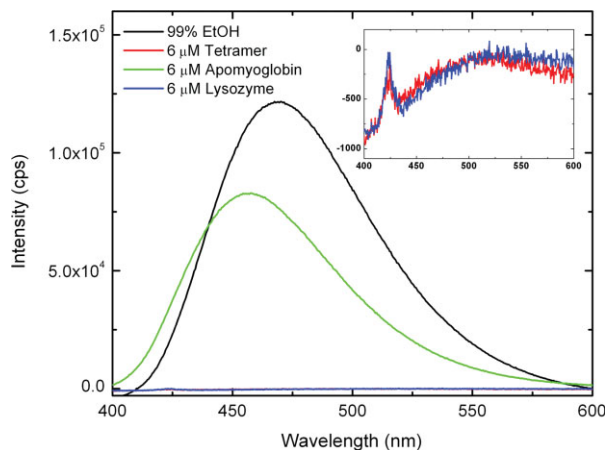


**Figure 4.** Fluorescence analysis of 1-anilino-naphthalene-8-sulfonate (ANS) binding. Protein samples were measured in 10 mM sodium phosphate, pH 7.5, and 150 mM NaCl. All samples contained 1  $\mu$ M ANS. Samples: 90% ethanol (black); 6  $\mu$ M apomyoglobin (green); 6  $\mu$ M lysozyme (red); 6  $\mu$ M ecE/ecK (blue).

disulfide crosslinking pattern between the cysteines in a mixture containing ecE and both of the cysteine-modified ecK peptides, one can distinguish between structures containing parallel helices vs. antiparallel helices. In the case of parallel helices, the amino termini would segregate at one end of the long axis of the coiled coil, and likewise, the carboxy termini would segregate at the other end. Thus, we would expect to find only crosslinked homodimers (ecK<sub>NN</sub> and ecK<sub>CC</sub>). For an antiparallel structure, where one would find both amino and carboxy termini in close proximity, we would expect heterodimers (ecK<sub>NC</sub>). In the work by Lumb and Kim, they found a lack of helix orientation specificity since they saw evidence for all three species in their mixtures.<sup>5</sup> As a control, we first looked for individual homodimers by mixing the ecE peptide with either ecK<sub>N</sub> or ecK<sub>C</sub> under native redox conditions. The redox conditions were set up so that the peptide interactions were driven by noncovalent interactions and so that disulfide crosslinking would not influence the distribution of structural states. Mixtures were analyzed by MALDI-TOF mass spectrometry to test for the expected homodimers (Table III), and the experimentally determined masses were essentially identical to the theoretical masses of the homodimers. When all three peptides were mixed together under native conditions, we only see evidence for homodimers, suggesting that the coiled-coil structures are predominantly parallel with respect to the helices. To be certain that there was no artifactual suppression of the expected heterodimer in the MALDI-TOF analysis, we also tested for disulfide crosslinking under somewhat denaturing conditions. In the presence of urea, we were able to detect all three species, including a well-defined mass for the heterodimer (Table III). It is

interesting to note that Lumb and Kim only report redox reactions in the presence of GuHCl, in which they also reported a lack of helix orientation specificity<sup>5</sup>; we wonder if they would have seen specificity of helix orientation under native conditions. Why slight destabilization of coiled-coil structures should result in a loss of helix orientation specificity is an interesting question and cannot be easily explained.

Heterospecificity of helix pairing can be engineered into coiled coils by taking advantage of electrostatic repulsions in homomeric structures (termed “negative design”),<sup>18</sup> electrostatic attractions in heteromeric structures, or both.<sup>19–21</sup> It is likely that charge repulsion plays a role in destabilizing the ecE and ecK homotetramers since, in both cases, the peptides are largely unfolded (see Fig. 2) under conditions in which the parent sequence is quite stable.<sup>10</sup> Evidence for interhelical electrostatic repulsion between charged residues at *c* and *e'* sites in ecE and ecK homotetramers was measured by studying the pH dependence of stability using CD as a probe. We would expect that charge neutralization of glutamates at low pH or lysines at high pH would result in stabilization of coiled-coil tetramers. It was found that ecE indeed underwent a folding transition as the pH was lowered below 6 with an apparent  $pK_a$  of the transition being 5.7 (see Fig. 5). The ecK peptide underwent a folding transition in basic conditions and was fully folded at pH 10 with an apparent  $pK_a = 9.4$ . Both ecE and ecK had apparent  $pK_a$  values for glutamate and lysine that were shifted when compared with their unperturbed  $pK_a$  values (glutamate  $pK_a = 4.3$ ; lysine  $pK_a = 10.5$ ), suggesting that neighboring charge effects are favoring the neutral forms of both amino acids in the resultant homotetrameric structures.

In addition to testing whether unfavorable electrostatic interactions between *e* and *c* site amino acids could disfavor homotetramer formation, we also asked whether the heterotetramer was stabilized by electrostatic attractions between the oppositely charged lysine and glutamic acid residues. Simple addition of NaCl, even up to molar concentrations, was insufficient to

**Table III.** MALDI-TOF Analysis of Redox Reactions Involving ecE, ecK<sub>N</sub>, and ecK<sub>C</sub>

Reaction <sup>a</sup>	Theoretical molecular mass <sup>b</sup>	MALDI-TOF molecular mass
ecK <sub>N</sub> alone	7607 Da	7605 Da
ecK <sub>C</sub> alone	7321 Da	7334 Da
ecK <sub>N</sub> + ecK <sub>C</sub>	7607, 7321, 7464 Da	7605, 7319 Da
ecK <sub>N</sub> + ecK <sub>C</sub> <sup>c</sup>	7607, 7321, 7464 Da	7601, 7467, 7318 Da

<sup>a</sup> Reactions were performed under redox control in the presence of ecE peptide. Only the homodimers are expected in the first two reactions.

<sup>b</sup> Theoretical MWs of disulfide-crosslinked homodimers/heterodimers in the order: ecK<sub>NN</sub>, ecK<sub>CC</sub>, ecK<sub>NC</sub>.

<sup>c</sup> Carried out in 2M urea.

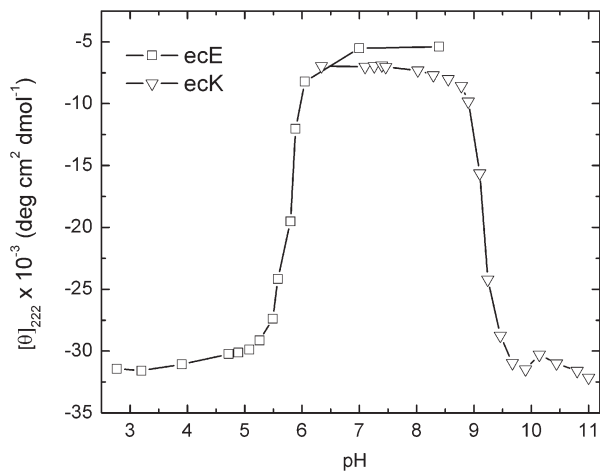


**Figure 5.** pH dependence on folding of 3  $\mu\text{M}$  ecE and ecK separately measured by CD signal at 222 nm, in 1 mM each of sodium phosphate, sodium borate, and sodium citrate and 150 mM NaCl.

destabilize the heterotetramer, presumably because the hydrophobic core plays a large role in the overall stability. We attempted a temperature dependent denaturation experiment in the presence and absence of 150 mM NaCl (this concentration is sufficient to largely shield solvated electrostatic attractions between side-chains). The tetramer remained fully folded over the entire testable temperature range under both salt conditions ( $T_M > 98^\circ\text{C}$ , data not shown), which made it impossible to resolve the contribution of electrostatics to the tetramer stability using this denaturation approach. Instead, we switched to chemical denaturation and found that urea could be used to unfold the heterotetramer. The midpoint of denaturation, in the absence of any salt, was about 5.8M (see Fig. 6). Upon addition of 150 mM NaCl, the coiled coil was significantly destabilized, with a midpoint around 3.5M urea, demonstrating that favorable electrostatic interactions must be assisting in stabilizing the heterotetramer.

We fit our data for ecE/ecK with a simple two-state thermodynamic model in order to extract free energies in the presence and absence of 150 mM NaCl. We found that, in the presence of 150 mM NaCl, the free energy was  $-28.5 \pm 0.9 \text{ kcal mol}^{-1}$  of tetramer ( $m = 0.78 \text{ kcal mol}^{-1} M^{-1}$ ) and compares favorably with that observed previously for a GCN4-derived heterotetramer.<sup>5</sup> The only other heterotetramer coiled coil that we are aware of is from our previous work on a shorter sequence that forms an antiparallel coiled coil, based on the tetramerization domain of the Lac repressor, and we reported its stability as being  $-24.0 \text{ kcal mol}^{-1}$ . In the absence of NaCl, the stability of ecE/ecK increased to  $-31.1 \pm 0.4 \text{ kcal mol}^{-1}$  ( $m = 0.77 \text{ kcal mol}^{-1} M^{-1}$ ), yielding a modest  $\Delta\Delta G$  of 2.6  $\text{kcal mol}^{-1}$  upon change in salt concentration. Assuming that all of the charged residues are engaged in electrostatic interactions, the change in  $\Delta G$  per ion

pair is only  $0.16 \text{ kcal mol}^{-1}$  upon the addition of salt. This does not imply that the electrostatic interactions are fully screened because it is possible that partial desolvation of the charges could lead to incomplete screening with 150 mM NaCl. In contrast, the difference in stability between 0.0 and 0.1M NaCl for the designed Lac repressor heterotetramer was  $7.4 \text{ kcal mol}^{-1}$ . We interpreted this large difference as owing to greater solvation due to placement of the charged residues in the more solvated *b* and *c* heptad positions.

## Materials and Methods

### Modeling

Replacement of native residues with either glutamate or lysine in the GCN4 p-LI structure (1GCL) were made using InsightII 2000 (Biosym Technologies). The new side chains were manually adjusted to allow close juxtaposition of the lysine amino groups and the glutamate carboxyl groups between the neighboring helices. After manual adjustment, the sidechains were subjected to molecular mechanics energy minimization using the Discover module to remove steric clashes. Energy minimization involved 5000 iterations of steepest descents using a dielectric of 1.0 in which the backbone conformation was kept fixed.

### Peptide synthesis and purification

The synthesis of ecE and ecK was carried out on an Applied Biosystems 433A peptide synthesizer (Perseptive Biosystems) using standard fluorenyl methoxycarbonyl chemistry and using PAL resin (Advanced ChemTech), which provides an amide at the carboxy-terminus. The peptides were acetylated at the amino terminus prior to trifluoroacetic acid (TFA) cleavage. Peptides were purified using reversed phase-high performance liquid chromatography (RP-HPLC) with a mobile phase of water and acetonitrile with 0.1% TFA

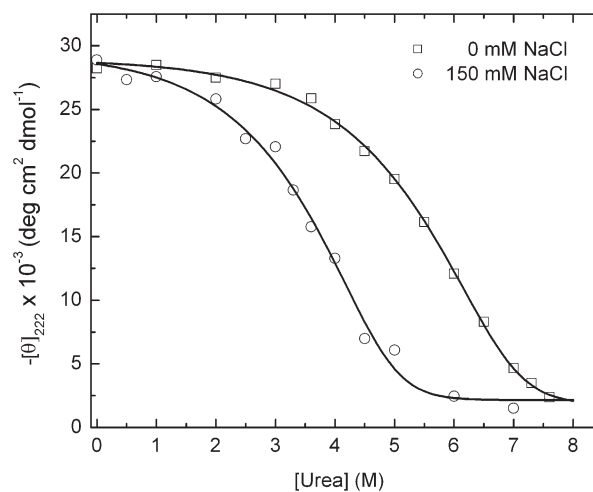


**Figure 6.** Denaturation profile of ecE/ecK mixture in 10 mM sodium phosphate, pH 7.5 with and without 150 mM NaCl at  $25^\circ\text{C}$  as monitored by circular dichroism.

on a Varian ProStar system equipped with a Varian Dynamax semi-preparative C18 column. Peptide identities were confirmed using MALDI-TOF mass spectrometry yielding molecular masses of 3441.2 Da (theoretical molecular mass = 3443.4 Da) for ecE and 3450.3 Da (theoretical molecular mass = 3450.9 Da) for ecK. Peptides were lyophilized and dissolved in MilliQ-treated water to make stock solutions. Concentration of stocks was determined by measuring the absorbance of the tyrosine residue in 6M GdnHCl.<sup>15</sup>

### **Redox analysis of helix orientation**

Helix orientation was determined by adapting a redox method for disulfide crosslinking of helix pairs developed by the Kim lab.<sup>5</sup> Variants of the ecK peptides were synthesized containing either a Trp-Cys-Gly-Gly at the N terminus (ecK<sub>N</sub>) or a Gly-Gly-Cys at the C terminus (ecK<sub>C</sub>). The peptide identities were confirmed by MALDI-TOF mass spectrometry, yielding molecular mass of 3803.5 Da (theoretical molecular mass = 3803.5 Da) for ecK<sub>N</sub> and 3659.5 Da (theoretical molecular mass = 3660.5 Da) for ecK<sub>C</sub>. Redox reactions for all mixtures of the ecK derivatives with ecE were carried out in 50 mM Tris-HCl, pH 8.7, 150 mM NaCl, 25 mM oxidized glutathione, 50 mM reduced glutathione, and 0.1% NaN<sub>3</sub>, as described previously<sup>5</sup> in the presence or absence of 2M urea. Reactions were incubated overnight at 25°C under a constant stream of nitrogen to maintain the redox conditions and quenched with 10% acetic acid. The products were then purified by RP-HPLC using a Varian Microsorb 100-5 C18 250 × 4.6 mm column and analyzed by MALDI-TOF mass spectrometry to probe for disulfide crosslinking involving homodimers (ecK<sub>NN</sub> and ecK<sub>CC</sub>) or heterodimers (ecK<sub>NC</sub>).

### **Circular dichroism spectropolarimetry**

CD measurements were taken on an Aviv circular dichroism spectropolarimeter (Model 202-01). Spectra were collected using a 0.1-cm pathlength cuvette at 25°C using a bandwidth of 1.00 nm, 0.5-nm step size, and 3-s averaging time, and using an average of three scans. pH dependence and urea denaturation measurements were measured by time-averaging at least 30 s at 222 nm. The pH measurements were made using a buffer system containing 1 mM each of sodium phosphate, sodium borate, and sodium citrate, with 150 mM NaCl in a 1-cm pathlength cuvette. The pH changes were measured inside the cuvette directly by using an MI-710 combination pH electrode (Microelectrodes).

### **Fluorescence spectroscopy**

ANS fluorescence was measured using a Spex Fluorolog using an excitation wavelength of 370 nm. Spectra were taken at room temperature using a 1-cm pathlength cuvette, an increment of 1 nm, and a 15-s averaging time. Protein samples were at a 6 μM con-

centration with 1 μM ANS and 10 mM sodium phosphate buffer, pH 7.5.

### **Analytical ultracentrifugation**

Sedimentation equilibrium (SE) and sedimentation velocity (SV) experiments were performed using six- or two-channel Epon charcoal-filled centerpieces, respectively, in a Beckman ProteomeLab XL-A analytical ultracentrifuge equipped with an An60Ti rotor. Samples for SE experiments were run at 30,000, 40,000, and 50,000 rpm at 25°C using 30 μM peptide in 10 mM phosphate, pH 7.3, with 150 mM NaCl. Equilibrium data were truncated using the WinReedit (v. 0.999) program (©1998) and analyzed using WinNonLin (v. 1.035; ©1997).<sup>22</sup> Temperature-corrected partial specific volumes (ecE = 0.7517 mL g<sup>-1</sup>; ecK = 0.8004 mL g<sup>-1</sup>; ecE/ecK = 0.7760 mL g<sup>-1</sup>), solution density (1.00586 g mL<sup>-1</sup>), and solution viscosity (1.0206 × 10<sup>-2</sup> Pa s) were computed using SednTerp, v 1.08.<sup>23</sup>

SV data were run with 400 μM ecE/ecK under the same buffer conditions as the SE experiments. The rotor temperature was equilibrated to the running temperature (20°C) prior to spinning of the rotor. Data were collected at a rotor speed of 50,000 rpm using an absorbance of 278 nm. Absorbance scans were collected using a delay of time 0 s and a radial step size of 0.003 cm. SV data were analyzed using the DCDT+ program (v. 2.0.9, John Philo, Thousand Oaks, CA). Scans near the bottom of the column were used for data analysis using DCDT+ with the constraint being that the plateau absorbance at the bottom of the column was well defined. The number of sedimentation profiles used for analysis with this program was defined by the constraints specified by the algorithm in order to avoid boundary spreading due to diffusion. Molecular masses and the standard errors for analyzed species were calculated from best fit  $s_{20,w}$  and  $D_{20,w}$  values using DCDT+.

### **Conclusions**

To increase the toolkit of structures that can self-assemble into large-scale biomaterials, we designed a parallel coiled-coil heterotetramer that could form highly stable structures driven by electrostatic interactions. Redesign strategies, similar to that taken by Woolfson and coworkers,<sup>3,24</sup> could lead to favoring offset helical interactions that would template the assembly of self-assembling polymers. Toward this goal, we introduced either glutamates or lysines at *c* and *e* heptad positions in a peptide sequence that specifies highly stable parallel coiled-coil tetramers, called GCN4 p-LI.<sup>10</sup> We chose these heptad positions because modeling suggested that glutamates and lysines could interact to form salt bridges and these interactions would be sufficiently desolvated to resist screening by physiological amounts of salt. Consistent with this strategy, we found that either the acidic or the basic peptide alone is severely destabilized relative to the

parent sequence whereas an equal mixture of the two has comparable stability to two other heterotetramer model systems.<sup>4,5,14</sup> In addition, physiological salt concentration has only a modest destabilizing affect on stability, indicating a robust design for future work. Thus, these results show great promise for the creation of “smart” materials whose assembly could be regulated by environmental factors, such as NaCl and pH, as demonstrated here.

### Acknowledgments

The authors thank Jeff Jopling for technical assistance in the work. The authors also thank William DeGrado for the use of his MALDI-TOF mass spectrometer.

### References

1. Fairman R, Akerfeldt KS (2005) Peptides as novel smart materials. *Curr Opin Struct Biol* 15: 453–463.
2. Woolfson DN (2005) The design of coiled-coil structures and assemblies. *Adv Protein Chem* 70: 79–112.
3. Woolfson DN, Ryadnov MG (2006) Peptide-based fibrous biomaterials: some things old, new and borrowed. *Curr Opin Chem Biol* 10: 559–567.
4. Fairman R, Chao HG, Lavoie TB, Villafranca JJ, Matsueda GR, Novotny J (1996) Design of heterotetrameric coiled coils: evidence for increased stabilization by Glu(–)-Lys(+) ion pair interactions. *Biochemistry* 35: 2824–2829.
5. Lumb KJ, Kim PS (1995) A buried polar interaction imparts structural uniqueness in a designed heterodimeric coiled coil. *Biochemistry* 34: 8642–8648.
6. Lumb KJ, Kim PS (1998) A buried polar interaction imparts structural uniqueness in a designed heterodimeric coiled coil. *Biochemistry* 37: 13042.
7. Sia SK, Kim PS (2001) A designed protein with packing between left-handed and right-handed helices. *Biochemistry* 40: 8981–8989.
8. Alberti S, Oehler S, von Wilcken-Bergmann B, Muller-Hill B (1993) Genetic analysis of the leucine heptad repeats of Lac repressor: evidence for a 4-helical bundle. *EMBO J* 12: 3227–3236.
9. Krylov D, Mikhailenko I, Vinson C (1994) A thermodynamic scale for leucine zipper stability and dimerization specificity: e and g interhelical interactions. *EMBO J* 13: 2849–2861.
10. Harbury PB, Zhang T, Kim PS, Alber T (1993) A switch between two-, three-, and four-stranded coiled coils in GCN4 leucine zipper mutants. *Science* 262: 1401–1407.
11. Hill RB, Raleigh DP, Lombardi A, DeGrado WF (2000) De novo design of helical bundles as models for understanding protein folding and function. *Acc Chem Res* 33: 745–754.
12. Handel TM, Williams SA, DeGrado WF (1993) Metal ion-dependent modulation of the dynamics of a designed protein. *Science* 261: 879–885.
13. Walshaw J, Woolfson DN (2003) Extended knobs-into-holes packing in classical and complex coiled-coil assemblies. *J Struct Biol* 144: 349–361.
14. Vu C, Robblee J, Werner KM, Fairman R (2001) Effects of charged amino acids at b and c heptad positions on specificity and stability of four-chain coiled coils. *Protein Sci* 10: 631–637.
15. Pace CN, Vajdos F, Fee L, Grimsley G, Gray T (1995) How to measure and predict the molar absorption coefficient of a protein. *Protein Sci* 4: 2411–2423.
16. Rohl CA, Baldwin RL (1998) Deciphering rules of helix stability in peptides. *Methods Enzymol* 295: 1–26.
17. Roy S, Ratnaswamy G, Boice JA, Fairman R, McLendon G, Hecht MH (1997) A protein designed by binary patterning of polar and nonpolar amino acids displays native-like properties. *J Am Chem Soc* 119: 5302–5306.
18. Lumb KJ, Kim PS (1995) Measurement of interhelical electrostatic interactions in the GCN4 leucine zipper. *Science* 268: 436–439.
19. Yu Y, Monera OD, Hodges RS, Privalov PL (1996) Ion pairs significantly stabilize coiled-coils in the absence of electrolyte. *J Mol Biol* 255: 367–372.
20. Krylov D, Barchi J, Vinson C (1998) Inter-helical interactions in the leucine zipper coiled coil dimer: pH and salt dependence of coupling energy between charged amino acids. *J Mol Biol* 279: 959–972.
21. Marti DN, Jelesarov I, Bosshard HR (2000) Interhelical ion pairing in coiled coils: solution structure of a heterodimeric leucine zipper and determination of pKa values of Glu side chains. *Biochemistry* 39: 12804–12818.
22. Johnson ML, Correia JJ, Yphantis DA, Halvorson HR (1981) Analysis of data from the analytical ultracentrifuge by nonlinear least-squares techniques. *Biophys J* 36: 575–588.
23. Laue TM, Shah BD, Ridgeway TM, Pelletier SL, Computer-aided interpretation of analytical sedimentation data for proteins. In: Harding SE, Rowe AJ, Horton JC, Eds. (1992) *Analytical ultracentrifugation in biochemistry and polymer science*. Cambridge: The Royal Society of Chemistry. pp 90–125
24. Pandya MJ, Spooner GM, Sunde M, Thorpe JR, Rodger A, Woolfson DN (2000) Sticky-end assembly of a designed peptide fiber provides insight into protein fibrillogenesis. *Biochemistry* 39: 8728–8734.